RSC Advances

PAPER

View Article Online
View Journal | View Issue

Cite this: *RSC Adv.*, 2015, **5**, 88414

Stretchable, transparent and molecular permeable honeycomb electrodes and their hydrogel hybrids prepared by the breath figure method and sputtering of metals†

Hiroshi Yabu,*[a] Kuniaki Nagamine,[b] Jun Kamei,[a] Yuta Saito,[a] Taiki Okabe,[b] Tatsuaki Shimazaki[b] and Matsuhiko Nishizawa*[b]

Received 5th September 2015
Accepted 10th October 2015

DOI: 10.1039/c5ra18063e

www.rsc.org/advances

We here describe a thin, highly stretchable transparent and molecular permeable porous electrode with a well-defined honeycomb structure fabricated by a combination of a bottom-up breath figure process and top-down sputtering of metals. Furthermore, the honeycomb electrode–hydrogel hybrids show higher durability, optical transparency, and electrical conductivity. The optical and electrical properties of the electrode, and its potential for use as a stretchable transparent electrode, are discussed.

Introduction

Strong demand for wearable and implantable electrical devices has encouraged researchers to develop new types of conductive electrodes. Freestanding electrodes exhibiting high conductivity, mechanical elasticity, optical transparency and molecular permeability are required for integrating biosensors onto biological surfaces for continuous health monitoring.[1] In particular, optical transparency is imperative for electrodes used in contact lenses and other surface applications[2] requiring external light sensing. Molecular permeability is also important for sensor electrodes to sense biological molecules.[3]

A state-of-the-art top-down approach has been employed to realize stretchable electrodes. For example, Rogers and co-workers reported tattoo-like thin patterned metal meshes integrated with radiofrequency tags prepared by lithographic techniques.[4,5] Although these electrodes can be used as stretchable electrodes for sensing, they are obviously visible, and cannot be used for contact lenses and are less suited to continuous health monitoring of eyes and other organs, which are required transparency. To realize optical transparency of such mesh electrodes, elaborative miniaturization of the line width of mesh is required.

Several bottom-up strategies for creating stretchable transparent electrodes have also been reported. Metal nanowires and carbon nanotubes, which have high aspect ratios, have been embedded in stretchable matrices to provide conductive electrodes.[6,7] When the concentration of nanowires reaches the percolation limit, the nanowires connect to each other, providing an electron conduction passage. Hu *et al.* reported stretchable transparent electrodes prepared by spraying carbon nanotubes onto stretchable polymer films. However, the transparency of these electrodes (transmittance lower than 60%) was insufficient and the resistance dramatically increased as the number of stretch cycles increased.[8] Silver and copper nanowires have also been used to prepare transparent, stretchable electrodes.[9–11] However, dispersing nanowires homogeneously into and/or onto stretchable matrices (which are usually synthetic hydrophobic rubbers) without aggregation remains challenging; this is important because aggregation results in optical scattering, making the film opaque. Graphene is one of the most attractive materials for creating transparent and stretchable electrodes[12] but it is too rigid for use in stretchable electronics, which require a high elongation ratio.

Porous electrodes prepared by templating polystyrene spheres,[13] anodic aluminum oxides[14] or conventional photolithography[15] have also been employed to prepare transparent electrodes, however, it is difficult to achieve stretchability and elaborate multiple processes to develop porous electrodes including photolithographic processes, form arrays of polystyrene spheres and electrodes, and removal of template polystyrene spheres are required. Furthermore, to the best of our knowledge, there is no report achieving stretchable, transparent and molecular permeable freestanding electrodes.

[a]*Institute of Multidisciplinary Research for Advanced Materials (IMRAM), Tohoku University, 2-1-1, Katahira, Aoba-Ku, Sendai 980-8577, Japan. E-mail: yabu@tagen.tohoku.ac.jp*

[b]*Department of Bioengineering and Robotics, Tohoku University, 6-6-1, Aoba, Sendai 980-8579, Japan*

† Electronic supplementary information (ESI) available: Experimental set up of resistance measurement, SEM images of Ti and Pt sputtered honeycomb electrodes, sputtering rate of Au, EDX spectrum, S–S curve, cross-sectional TEM of Au sputtered honeycomb films, and ink permeation experiment video are available as ESI. See DOI: 10.1039/c5ra18063e

We previously reported honeycomb-patterned polymer films (honeycomb films) generated using condensed water droplets during film preparation from polymer solutions.[16] The surface of the solution cools during solvent evaporation due to evaporative cooling and water microdroplets spontaneously condense onto the surface of the solution.[17] Complete evaporation of the solvent provides a microporous film with hexagonal arrangements. Porous electrodes have been prepared by electroless deposition of silver onto polystyrene honeycomb films.[18] However, due to the thick metal film formation, the film did not transmit the light anymore and the film became too rigid to bend with keeping its conductivity. Such a film can not be used for transparent stretchable and molecular permeable electrodes. Recently, we found that honeycomb films of 1,2-polybutediene (PB) are highly stretchable due to their high porosity and viscoelastic nature,[19] and pores provide an optical path and high transparency. The properties of PB honeycomb film suggest it is a good candidate as a substrate for stretchable, transparent electrodes.

We here describe a thin, flexible, highly stretchable and transparent porous electrode with a well-defined honeycomb structure fabricated by a combination of a bottom-up breath figure process and top-down sputtering of metals. The optical and electrical properties of the electrode, and its potential for use as a stretchable transparent electrode, are discussed.

Experimental section

Preparation of 1,2-poly(butadiene) (PB) honeycomb films

PB (RB-820) was kindly provided by JSR Co., Ltd. (Tokyo). PB honeycomb films were prepared according to the literature.[19] Typically, PB was dissolved in chloroform to prepare a 10 mg mL^{-1} solution by adding a small amount (1 mg mL^{-1}) of amphiphilic copolymer (Polymer 1).[18] The solution (40 mL) was cast onto a glass substrate, then humid air (over 90% relative humidity) was blown onto the surface. After complete evaporation of the solvent and template water droplets, the honeycomb film was suspended in ethanol, placed on a 50 mm × 50 mm polyethylene terephthalate (PET) frame, and dried at room temperature.

Formation of metal layers on the PB honeycomb films

Au, Ti, and Pt were sputtered onto PB honeycomb films for between 10 s to 60 s using a vacuum deposition system (SVC-700TMSG/Adexcel, Sanyu Electron Co., Ltd., Tokyo). References were generated by coating PB honeycomb films with Au using a resistively heated vacuum-evaporation system (VPC-260F, ULVAC KIKO Inc., Tokyo).

Formation of metal-coated PB honeycomb films on flexible substrates

Poly(dimethylsiloxane) (PDMS) elastomer and a hydrogel were used as flexible substrates. PDMS was prepared by mixing a catalyst into prepolymer (mixing ratio = 1/15), then cast into a mold (200 mm × 200 mm × 0.5 mm). The prepolymer was cured at 60 °C for 3 h. The cured PDMS was removed from the mold and cut into 10 mm × 30 mm sheets. Honeycomb electrodes were fixed onto the surfaces of PDMS sheets and used for stretch-resistance measurements. A double network (DN) hydrogel was prepared using previously reported protocols.[20] A prepolymer solution was prepared containing 1 M 2-acrylamido-2-methyl-1-propanesulfonic acid sodium salt (NaAMPS, Sigma Aldrich Japan, Tokyo) as a monomer, 40 mM *N*,*N*′-methylenebis(acrylamide) (MBAA, Wako Pure Chemicals, Wako, Saitama, Japan) as a crosslinker, and 1 mM 2-oxoglutaric acid (Wako Pure Chemicals) as a photoinitiator. This solution was poured into a reaction chamber composed of two glass plates separated by a 0.2 mm thick silicone spacer. The reaction chamber was irradiated with UV light (365 nm, 8 W, Funakoshi, Tokyo) for 6 h in a nitrogen-filled glovebox. The obtained PNaAMPS hydrogel sheet was immersed in an aqueous solution containing 3 M *N*,*N*-dimethylacrylamide (DMAAm, Sigma Aldrich), 3 mM MBAA, and 1 mM 2-oxoglutaric acid for 2 days at room temperature in the dark. The hydrogel sheet was again irradiated with UV light for 6 h in the nitrogen-filled glovebox to polymerize the second hydrogel, followed by washing with distilled water overnight to remove residual cytotoxic monomers. The resulting DN hydrogel was about 0.5 mm thick after swelling in distilled water.

Au, Ti, and Pt were sputtered onto PB honeycomb films for between 10 s to 60 s using a vacuum deposition system (SVC-700TMSG/Adexcel, Sanyu Electron Co., Ltd., Tokyo). References were generated by coating PB honeycomb films with Au using a resistively heated vacuum-evaporation system (VPC-260F, ULVAC KIKO Inc., Tokyo).

Laser patterning

The Au-sputtered PB honeycomb film was laminated onto the surface of the DN hydrogel sheet or a commercial soft contact lens (SEED). Then, the film on the hydrogels was cut into desired patterns using a CO_2 laser cutter (Versa LASER, Universal Laser Systems, Scottsdale AZ) operated at 30 mW and 1% of the maximum cutting speed to minimize damage to the hydrogel substrate.

Analysis

The thicknesses of the deposited Au thin films were measured by transmission electron microscopy. Cross-sectional specimens 100 nm thick were prepared by embedding a sample film in epoxy resin (EPOC) and cutting with an ultramicrotome (UC-6, Lica, Jena, Germany). The slices were observed by transmission electron microscopy (TEM, H-7650, Hitachi, Ltd., Hitachi, Japan) and the thicknesses of the Au films were measured from the cross-sectional TEM images using image analysis software (Image J, National Institutes of Health, Bethesda, MD). Elemental analysis was performed by electron dispersive X-ray spectroscopy (EDS) using an EDAX EDS unit. The surface structures of the honeycomb electrodes were observed using a scanning electron microscope (S-5200, Hitachi, Ltd.) after sputtering a thin film of Os to ensure electrical conductivity. Relation between elongation ratio and strain of a PB honeycomb film and a Au sputtered PB honeycomb films

were measured by using a tensile tester (DPU, IMADA, Toyohashi). Details of the experimental setup for measuring resistance are shown in ESI S-1.† The two ends of a honeycomb electrode fixed on a PDMS sheet were generally clamped onto mobile stages and stretched unidirectionally. Current values were simultaneously measured by applying 1 V across the electrodes during stretching using a potentiostat and the change in resistance was calculated using Ohm's law ($R = V/I$, where R, V and I are resistance, voltage and current, respectively). The sheet resistance of a honeycomb electrodes and hydrogel hybrid was also measured 4-point probe method by using a resistivity meter (MCP-T610, Loresta GP, Mitsubishi Chemical Analytech, Co. Ltd., Tokyo). The stabilities of the honeycomb electrodes were evaluated by measuring changes in their resistance by applying repeated 30–50% strains. Molecular permeability was examined by put a drop of ink solution (Pelikan4001, Fountain Pen Ink) onto the surface of honeycomb electrode and hydrogel hybrids. The optical transparencies of 10 mm × 10 mm specimens were measured using a diffuse reflectance spectrometer (V-670 equipped with a diffuse reflectance spectroscopy unit, Jasco, Tokyo).

Results and discussion

Fig. 1(i)–(iii) show schematic illustrations of the honeycomb electrodes and honeycomb electrode hydrogel hybrids. PB honeycomb films with 5 μm pores were prepared by casting a chloroform solution of PB and Polymer 1 under humid conditions, according to the literature.[21] The PB honeycomb film was transferred to a PET frame and metal (Au, Pt, or Ti) was sputtered onto the surface (see ESI, S-2†) for different lengths of time. Although Pt and Ti samples also have low resistance values, we chose Au to make stretchable electrodes, since Pt and Ti were originally rigid comparing with Au. An SEM image (inset, Fig. 1) shows that the surface structure of the honeycomb film is retained after sputtering Au to provide the honeycomb electrode. The cross-sectional TEM images and EDX spectra show that a thin metal film formed only on the surface of the honeycomb films, and that the thickness of the metal film increased with increasing sputtering time at a growth rate of 0.52 nm s^{-1} (see ESI, S-3 and S-4†). As shown in the ESI S-5,† stress–strain curve of a Au sputtered PB honeycomb electrode was well stretched as well as original PB since the thicknesses of Au layer was very thin. The yield strength of the honeycomb electrode is much lower than that of original PB due to the porous structure.

Fig. 2(a) shows the relationship between stretch and sheet resistance of honeycomb electrodes sputtered with Au for different lengths of time. The sheet resistance of a honeycomb electrode prepared by 10 s of sputtering was over 5 MΩ sq^{-1}, showing that 10 s of sputtering is insufficient to form conductive passages on the surface of a honeycomb film. The sheet resistance of honeycomb electrodes prepared by sputtering Au for 30–60 s was initially low (around 300 Ω sq^{-1}), but suddenly increased following slight deformation (10–20% strain). On the other hand, honeycomb electrodes prepared by sputtering Au for 20 s retained a low sheet resistance of less than 600 Ω sq^{-1}, identical to the resistance of commercially available indium tin oxide (ITO) electrodes. The resistance of the honeycomb electrode gradually increased above 60% strain. Since human skin can deform up to 50%,[22] the stretch properties of the honeycomb electrode are suitable for use in epidermal electronics. Sputtering for 20 s resulted in Au overlapping particulates forming on the surface of the honeycomb film (see ESI S-5†). These Au particles remained overlapped during stretching, thus maintaining the electrical conductivity. On the other hand, sputtering for more than 30 s resulted in thicker Au films that easily fractured when mechanical stress was applied. Since the elongation of Au sputtered honeycomb electrode was over 500% (see ESI, S-5†), the resistance decrease was originated from breaking of metal layers and not from degradation of honeycomb structures. Vacuum thermal deposition of Au onto PB honeycomb films provided films that were insufficiently flexible for the same reason. The formation of thicker, dense metal films led to rigid honeycomb electrodes, indicating that the conductive paths were easy to damage by the application of small strains to the electrodes.

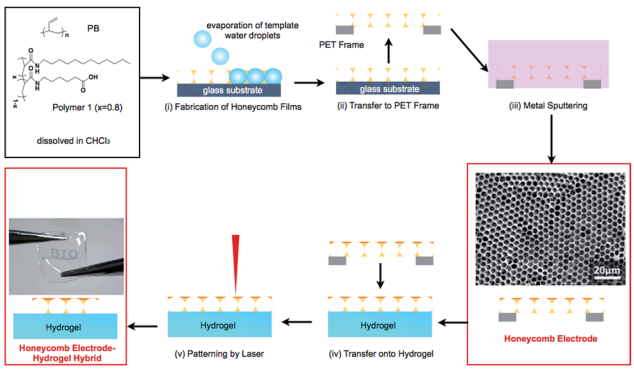

Fig. 1 Schematic illustration of the preparation of honeycomb electrodes and a honeycomb electrode–hydrogel hybrid. A SEM image of an Au-sputtered PB honeycomb electrode and a photograph of a honeycomb electrode–hydrogel hybrid are shown.

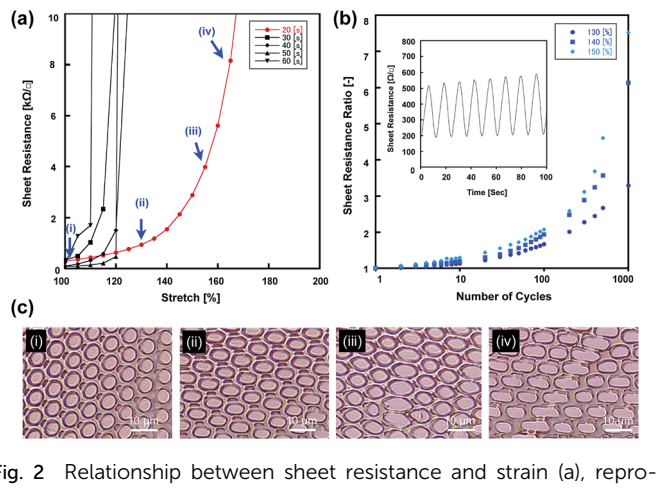

Fig. 2 Relationship between sheet resistance and strain (a), reproducibility of the sheet resistance after repeated stretching (b), and photographs of honeycomb electrode deformation (c).

Deformation of the honeycomb electrodes was observed by optical microscopy. The uniform hexagonal porous structure of a honeycomb electrode was observed prior to strain (Fig. 2(c)(i)), but the hexagonal structures deformed to ellipsoidal shapes during stretching (Fig. 2(c)(ii)), and some parts of the honeycomb frame broke when stretched above 60% (Fig. 2(c)(iii)). The sheet resistance gradually increased with further stretching (Fig. 2(c)(iv)) since the broken honeycomb network increased resistance.

Fig. 2(b) shows the change in sheet resistance during 1000 stretch–relax cycles with different degrees of strain (30–50%). The sheet resistance gradually increased, but it is noteworthy that the maximum sheet resistance at 30% stretch is 600 Ω sq^{-1} after 1000 cycles, which is low enough to use in sensor devices. These results indicate that honeycomb electrodes prepared by sputtering Au for 20 s exhibit high durability during repeated stretching.

The high flexibility and stretchability of honeycomb electrodes prepared by sputtering Au for 20 s suggested that they can be fixed onto flexible, swellable hydrogels. Fig. 3(a) shows honeycomb electrodes patterned to spell "BIO" on a hydrogel using a laser patterning technique. Surprisingly, the electrodes retained their structure after repeated swelling and deswelling of the hydrogel (Fig. 3(b)). Note that resistance of the honeycomb electrode and hydrogel hybrid measured by 4-point probe method was ranging from 20 Ω sq^{-1} to 100 Ω sq^{-1}, and the value did not change before and after swelling. Furthermore, this honeycomb electrode has high (over 90%) optical transparency at visible light wavelengths (Fig. 3(c)). The patterned electrode was difficult to see when placed over the logo of our university (inset images, Fig. 3(c)). This is noteworthy because the original optical aperture of the honeycomb films calculated from SEM images is less than 70%. We previously estimated that over 90% of light is transmitted though several nanometer-thick thin films due to optical pathways in the film.[23] As shown in ESI S-5,† since the formed Au film was approximately 20 nm thick, which is much less than the wavelength of visible light, the honeycomb structure should readily transmit light, as is indeed the case. The honeycomb electrode–hydrogel hybrids show higher durability, optical transparency, and electrical conductivity compared with the stretchable electrodes mentioned in the introduction. We previously reported a poly(3,4-ethylenedioxythiophene)/polyurethane (PEDOT–PU) electrode prepared on a hydrogel surface that can be used to monitor signals from biological bodies such as nerve cells.[24] However, that electrode is not transparent and so cannot be used on the eyes, skins and other organs. Moreover, honeycomb and hydrogel hybrids have molecular permeability. Since the original honeycomb films have pores pass through top to bottom surfaces, when a drop of ink solution was placed on the surface of the honeycomb film, ink solution diffused though the honeycomb film (see ESI, S-7†). In the case of a honeycomb film and hydrogel hybrid, ink molecules pass though the honeycomb pores and diffused into the hydrogel (Fig. 4). This result indicates that honeycomb electrodes can be exposed with the molecules pass though the hybrids. This property is imperative for sensing molecules from the biological bodies. Honeycomb electrodes with high transparency and stretchability will pave the way to realizing the continuous monitoring of the health of such organs.

Finally, we checked the applicability of honeycomb electrode–hydrogel hybrids. Fig. 5(a) shows a patterned honeycomb electrode placed on a contact lens surface. It is clear that the honeycomb electrode is soft enough to attach onto the surface of a contact lens. Furthermore, an LED lamp placed on the surface of a contact lens can be lit using the honeycomb electrodes (Fig. 5(b)), demonstrating the utility of honeycomb electrodes as stretchable transparent electrodes. Honeycomb electrode–hydrogel hybrids can be wrapped around a pen (Fig. 5(c)) or a finger (Fig. 5(d)), showing they can work as electrodes on surfaces other than contact lenses. It is noteworthy that resistance values of honeycomb electrodes and hydrogel hybrids measured on such curved surfaces by 4-points probe method were identical with original one, which was ranging from 20 Ω sq^{-1} to 100 Ω sq^{-1}, since the deformation induced by the curvature of a finger was smaller than that of the deswelled hybrid. The result means the honeycomb films and

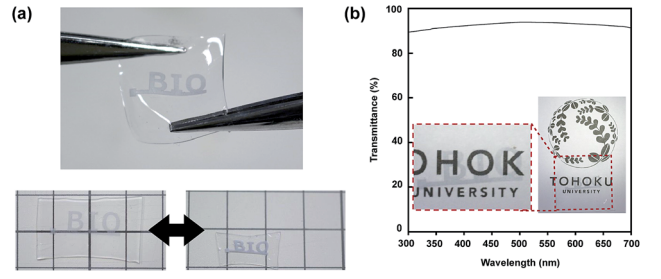

Fig. 3 Photographs of a patterned honeycomb electrode–hydrogel hybrid (a) and optical light transmittance of a honeycomb electrode–hydrogel hybrid (b).

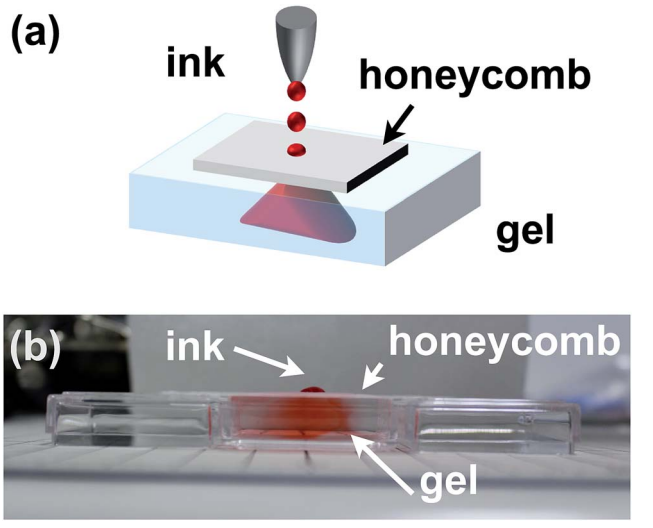

Fig. 4 Schematic illustration of molecular permeability experiment (a) and a side view of the experimental set up (b). Note that red ink has passed through the honeycomb and has diffused into the hydrogel.

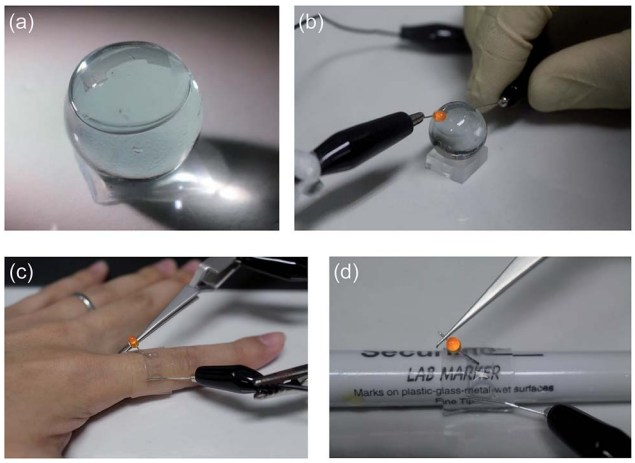

Fig. 5 Photographs of honeycomb electrodes and their hydrogel hybrids placed on a contact lens (a), (b), a finger (c) and a pen (d).

hydrogel hybrids have enough durability to adhere onto the curved surfaces.

Conclusions

We developed a new class of transparent stretchable honeycomb electrodes and their hydrogel hybrids that can be used to electrically wire a wide variety of surfaces. The honeycomb electrodes have high durability and high optical transparency, and can be used to create sensors on contact lenses, fingers, and other biological surfaces. These novel transparent stretchable electrodes open the way to the continuous sensing of various biological signals to provide continuous health monitoring.

Acknowledgements

We thank Mr Kouju Ito and co-workers Fujifilm Co. Ltd. for providing some of the PB honeycomb films used in this study. We also thank Ms Minori Suzuki for helping with the cross-sectional TEM observations of Au-sputtered PB honeycomb films. This work was partially supported by Grant-in-Aid for Challenging Exploratory Research (Grant No. 26620170) and the Center of Innovation Program, COI-Stream Project, Japan Science and Technology Agency (JST), Japan.

Notes and references

1 M. Vosgueritchian, D. J. Lipomi and Z. Bao, *Adv. Funct. Mater.*, 2012, **22**, 421–428.
2 N. M. Farandos, A. K. Yetisen, M. J. Monteiro, C. R. Lowe and S. H. Yun, *Adv. Healthcare Mater.*, 2014, **4**, 792–810.
3 S. Sekine, Y. Ido, T. Miyake, K. Nagamine and M. Nishizawa, *J. Am. Chem. Soc.*, 2010, **132**, 13174–13175.
4 D. H. Kim, *et al.*, *Science*, 2011, **333**, 838–843.
5 J. W. Jeong, *et al.*, *Adv. Mater.*, 2013, **25**, 6839–6846.
6 P. Lee, *et al.*, *Adv. Mater.*, 2012, **24**, 3326–3332.
7 L. Xiao, *et al.*, *Nano Lett.*, 2008, **8**, 4539–4545.
8 L. Hu, W. Yuan, P. Brochu, G. Gruner and Q. Pei, *Appl. Phys. Lett.*, 2009, **94**, 161108.
9 W. Hu, R. Wang, Y. Lu and Q. Pei, *J. Mater. Chem. C*, 2014, **2**, 1298–1305.
10 M.-S. Lee, *et al.*, *Nano Lett.*, 2013, **13**, 2814–2821.
11 R. M. Mutiso, M. C. S. herrott, A. R. Rathmell, B. J. Wiley and K. I. Winey, *ACS Nano*, 2013, **7**, 7654–7663.
12 G.-T. Kim, S.-J. Gim, S.-M. Cho, N. Koratkar and I.-K. Oh, *Adv. Mater.*, 2014, **26**, 5166–5172.
13 N. Kwon, K. Kim, S. Sung, I. Yi and I. Chung, *Nanotechnology*, 2013, **24**, 235205–235209.
14 H. Y. Jang, S.-K. Lee, S. H. Cho, J.-H. Ahn and S. Park, *Chem. Mater.*, 2013, **25**, 3535–3538.
15 W.-K. Kim, *et al.*, *Sci. Rep.*, 2015, 10715.
16 H. Yabu, M. Tanaka, K. Ijiro and M. Shimomura, *Langmuir*, 2003, **19**, 6297–6300.
17 O. Karthaus, *et al.*, *Langmuir*, 2000, **16**, 6071–6076.
18 H. Yabu, Y. Hirai and M. Shimomura, *Langmuir*, 2006, **22**, 9760–9764.
19 T. Kawano, *et al.*, *Biomacromolecules*, 2013, **14**, 1208–1213.
20 Y. M. Chen, *et al.*, *J. Biomed. Mater. Res., Part A*, 2009, **88**, 74–83.
21 H. Yabu and M. Shimomura, *Langmuir*, 2005, **21**, 1709–1711.
22 T. Yamada, *et al.*, *Nat. Nanotechnol.*, 2011, **6**, 296–301.
23 H. Yabu, T. Nakanishi, Y. Hirai and M. Shimomura, *J. Mater. Chem.*, 2011, **21**, 15154.
24 M. Sasaki, *et al.*, *Adv. Healthcare Mater.*, 2014, **3**, 1919–1927.